Published in final edited form as:
J Comp Neurol. 2005 October 31; 491(4): 320–329. doi:10.1002/cne.20704.

Stereological Estimation of the Number of Neurons in the Human Amygdaloid Complex

Cynthia Mills Schumann[1] and **David G. Amaral**[1,*]

[1]Department of Psychiatry and Behavioral Sciences and the M.I.N.D. Institute, University of California, Davis, Sacramento, CA 95817

Abstract

Pathological changes in neuronal density in the amygdaloid complex have been associated with various neurological disorders. However, due to variable shrinkage during tissue processing, the only way to unambiguously determine changes in neuron number is to estimate absolute counts, rather than neuronal density. As the first stage in evaluating potential neuropathology of the amygdala in autism, the total number of neurons was estimated in the control human amygdaloid complex using stereological sampling. The intact amygdaloid complex from one hemisphere of ten brains was frozen and sectioned. One 100 μm section was selected every 500 μm and stained by standard Nissl method. The entire amygdaloid complex was outlined then further partitioned into five reliably defined subdivisions: 1. lateral nucleus, 2. basal nucleus, 3. accessory basal nucleus, 4. central nucleus, 5. remaining nuclei (including anterior cortical, anterior amygdaloid area, periamygdaloid cortex, medial, posterior cortical, nucleus of the lateral olfactory tract, amygdalohippocampal area, and intercalated nuclei). The number of neurons was measured using an optical fractionator with Stereoinvestigator software. The mean number of neurons ($\times 10^6$) for each region was: lateral nucleus: 4.00, basal nucleus: 3.24, accessory basal nucleus: 1.28, central nucleus: 0.36, remaining nuclei: 3.33, total amygdaloid complex: 12.21. The stereological assessment of neuron number in the human amygdala provides an essential baseline for comparison of patient populations, such as autism, in which the amygdala may develop abnormally. To facilitate these types of analyses, this paper provides detailed anatomical description of the methods used to define subdivisions of the human amygdaloid complex.

Keywords

amygdala; neuropathology; stereology; autism; medial temporal lobe; anatomy

Change in neuronal density or neuron number in the human amygdaloid complex has been associated with the pathogenesis of various neurological and psychiatric disorders. For example, an increase in the density of neurons in portions of the amygdaloid complex has been reported in postmortem studies of autism (Bauman and Kemper, 1985; 1994). In contrast, the number of neurons may be decreased in disorders such as epilepsy (Hudson et al., 1993; Wolf et al., 1997; Thom et al., 1999), dementia (Herzog and Kemper, 1980; Scott et al., 1992), and Parkinson's disease (Harding et al., 2002).

Although these studies are often portrayed as indicating an increase in, or loss of, neurons, the observations from all of these studies are either qualitative or present estimates of neuronal density (neurons per unit volume) rather than absolute neuron number. Several

*Correspondence to: David G. Amaral, Ph.D., Address: The M.I.N.D. Institute, UC Davis Medical Center, 2825 50th Street, Sacramento, Ca 95817, Email: dgamaral@ucdavis.edu, Phone: (916) 703-0225, Fax: (916) 703-0287.
Associate editor: Joseph L. Price

studies, however, have pointed out the flaws in declaring that a brain region is pathological based solely on density measures. Haug (1994) found that the process of fixation, which removes water to preserve the tissue, results in differential shrinkage of brains at different ages; shrinkage was inversely proportional to age. Moreover, the effects of disease processes on tissue shrinkage are unknown. Stereological techniques have been applied to other areas of the human brain to accurately measure absolute neuron numbers (Pakkenberg and Gundersen, 1988; West and Gundersen, 1990; Pakkenberg and Gundersen, 1997; West and Slomianka, 1998; Andersen et al., 2003; Andersen et al., 2004; Korbo et al., 2004; West et al., 2004). Although there is now a general consensus that the only way to get an accurate measurement of neurons is to use stereological methods (Saper, 1996) and the only way to unambiguously determine pathology-related changes in the number of neurons is to estimate absolute neuron number, recent studies of the amygdaloid complex continue to assess the density of neurons rather than absolute neuron number (Bowley et al., 2002; Harding et al., 2002).

Little is known about how dysfunction of the amygdaloid complex may be related to the pathogenesis of human disorders or accompanying behavioral impairments. This is due, in part, to our incomplete understanding of the normal anatomy of the human amygdaloid complex. This study sought to measure the total number of neurons in five well-defined subdivisions of the human amygdaloid complex using systematic stereological sampling techniques. In order to facilitate the use of these techniques in future studies, this paper provides a detailed description of the guidelines used to define the subdivisions of the human amygdaloid complex.

Materials and Methods

Tissue processing

Brain tissue through the entire rostrocaudal extent of the amygdaloid complex from ten human cases was acquired for this study. Eight cases were acquired from the Brain and Tissue Bank for Developmental Disorders at the University of Miami School of Medicine in contract to the National Institute of Child Health and Development. Two cases were acquired from the Department of Pathology at the University of California, Davis School of Medicine. This study was approved by the Institutional Review Board of the University of California, Davis. Clinical characteristics of the ten cases are summarized in Table 1.

After removal of the brain from the skull, each brain was immersed in 10% buffered formalin for at least eight weeks prior to transfer to our laboratory. A proton-density weighted magnetic resonance imaging (MRI) scan was acquired on each of the ten brains with a 1.5 Tesla magnet at the UC Davis Imaging Research Center as previously described (Schumann et al., 2001). A four centimeter block containing the entire rostrocaudal extent of the amygdala (Figure 1) was cut from one hemisphere and returned to 10% buffered formalin at 4 degrees Celsius. The amygdala tissue block was placed into a cryoprotectant solution (10% glycerol for two days and 20% glycerol for five days) in preparation for freezing. The tissue block was frozen with 2-methyl butane (isopentane) and serially sectioned into six series of 50 μm thick sections and two series of 100 μm thick sections. One 100 μm series was stained with 0.25% thionin (standard Nissl method) for further analyses.

The amygdaloid complex was outlined on every 100 μm Nissl section in which it was present (approximately 20-25 sections per case). The amygdaloid complex was further partitioned into five subdivisions: 1. lateral nucleus, 2. basal nucleus, 3. accessory basal nucleus, 4. central nucleus, and 5. remaining nuclei. A tenet of design based stereological techniques is that the entire area of interest must be reliably sampled. The first four

individual nuclei could reliably be defined from case-to-case. Other regions of the amygdala, such as the periamygdaloid cortex, were highly variable across cases. Since a goal of this study was to get an estimate of total neuron number in the amygdala, all remaining regions of the amygdala were grouped into “remaining nuclei” that could be accurately outlined. Since there is no published protocol for outlining the entire human amygdala or its major subdivisions, a detailed description of our strategy is provided below.

Nissl-stained brightfield photomicrograph images (Figure 2) were acquired with a Nikon Photomacrography Multiphot system, the amygdaloid complex was outlined with Canvas 9 (ACD Systems Inc., Miami, FL), and images were adjusted for brightness and contrast with Adobe Photoshop 10 (Adobe systems Inc., San Jose, CA).

Definition of the human amygdaloid complex outer border

The rostral most section in which the amygdaloid complex was initially outlined was defined as the section in which the first appearance of either the lateral or basal nucleus occurred (Figure2a). In this section, the periamygdaloid cortex, anterior cortical nucleus, and/or paralaminar nucleus, if present, were included in the outline. In some cases, portions of what appeared to be the periamygdaloid cortex, anterior cortical nucleus, and/or paralaminar nucleus were present rostral to this section. But these regions were not clearly definable and therefore were not included in the amygdala outline.

The starting point of the outline was the dorsolateral point of where the medial surface of the temporal lobe curves laterally (Figure 2a). From this point, a line was drawn ventrolaterally, including the anterior cortical nucleus, to the top of the lateral nucleus (or basal nucleus if no lateral nucleus was present). One exception to the above occurred if the ventral claustrum extended into the temporal lobe dorsal to the lateral nucleus and ventral to the anterior cortical nucleus. If the cluster of neurons in this area appeared continuous with the ventral claustrum, it was excluded as part of the amygdala outline. The outline continued along the lateral and ventral borders of the lateral and basal nucleus, then extended to the medial surface of the brain at the semiannular sulcus. The outline was completed by drawing along the medial surface of the temporal lobe to the starting point.

In progressively more caudal sections, additional nuclei appeared within the amygdaloid complex (Figure 2b). These included the accessory basal nucleus, located dorsomedial to the basal nucleus, and the nucleus of the lateral olfactory tract, which was visible in some cases ventral to the anterior cortical nucleus. The anterior amygdaloid area was also present dorsal to the lateral nucleus and ventrolateral to the anterior cortical nucleus. The outline was drawn from the dorsolateral most point of the medial surface of the brain to the dorsal border of the anterior amygdaloid area, then ventrolateral to the dorsal most point of the lateral nucleus and completed as described above.

At midrostrocaudal levels through the amygdaloid complex, the anterior amygdaloid area was no longer present (Figure 2c). Fiber tracts cut across the dorsolateral portion of the lateral nucleus. The basal nucleus also developed a large dorsal portion that appeared separated from the rest of the nucleus due to fiber tracts. The central nucleus appeared dorsal to the basal and accessory basal nuclei. The anterior cortical nucleus was replaced by the medial nucleus on the medial surface of the brain. The amygdala also had scattered intercalated nuclei that were included in the outline. The outline was drawn from the same starting point to the dorsal most point of the central nucleus, around the lateral surface of the central nucleus, until its ventrolateral extent was reached. The outline was then drawn to the dorsal extent of the lateral or basal nucleus, whichever extended further dorsal, and completed as described above.

When the optic tract extended further laterally than the medial surface of the brain, or extended the same distance laterally, the starting point of the outline became the dorsolateral extent of the optic tract (Figure 2d). The outline extended laterally from the starting point, dorsal to the medial nucleus and ventral to the substantia innominata, to the dorsal extent of the central nucleus and completed as described above. At this level, the amygdala was bordered dorsomedially by the substantia innominata, dorsolaterally by white matter, and ventrally by the hippocampus. The amygdala formed a portion of the medial surface of the brain adjacent to the optic tract. The temporal horn of the lateral ventricle often appeared along the lateral border of the lateral nucleus. The hippocampus was clearly separated from the lateral and basal nucleus by the paralaminar nucleus and the temporal horn of the lateral ventricle. The lateral and basal nuclei decreased in size in subsequent caudal sections. The outline at this level was drawn as described above.

At the caudal extent of the amygdaloid complex (Figures 2e and f), the amygdalohippocampal area appeared ventromedial to the basal and accessory basal nuclei and ventrolateral to periamygdaloid cortex. The amygdalohippocampal transition area was present medial to the basal nucleus and ventral to the posterior cortical nucleus as a dorsomedial extension of the hippocampus, and was not included in the amygdala outline. The outline at the caudal extent of the amygdala was drawn essentially as just described above for adjacent rostral sections. The ventromedial limit of the amygdaloid complex was located just ventral to the posterior cortical nucleus and dorsal to the amygdalohippocampal transition area. Sections were outlined until both the basal and accessory basal nuclei could no longer be identified. Although some variable portion of central nucleus, amygdalohippocampal area, and/or posterior cortical nucleus may still be present in sections located caudal to the basal and accessory basal nuclei, these were not clearly definable and therefore not included within the outline.

Delineation of the lateral nucleus

The lateral and ventral boundaries of the lateral nucleus were previously defined in the process of making the amygdala outer border outline. To define the dorsal and medial border, a line was drawn from the dorsolateral extent of the lateral nucleus at the existing outline and extended medially until the basal nucleus was reached to form the dorsal border (Figure 2a). This point was identified in two ways: 1) the dorsal extent of the border between the lateral and basal nucleus was marked by white matter slightly dipping ventrally between the two nuclei and 2) neurons in the dorsal portion of the basal nucleus were larger and darker than those of the adjacent lateral nucleus. The outline continued ventrally between the lateral and basal nucleus until the existing outline of the amygdala was reached.

At midrostrocaudal levels, the dorsolateral division of the lateral nucleus extended further dorsal than in rostral sections (Figure 2c). The dorsal and medial outline was drawn as described above for rostral sections. The medial border of the lateral nucleus, particularly in the ventral portion, was difficult to define. In addition to the suggestions above, another aid to delineate the lateral and basal nuclei was to find where the paralaminar nucleus, along the existing ventral border of the amygdala, extended dorsally between the two nuclei.

In more caudal sections, the lateral nucleus continued to decrease in size and was less fragmented by fiber tracts (Figure 2d). The outline was drawn as described above until the last section in which lateral nucleus was present (Figure 2e).

Delineation of the basal nucleus

Most of the lateral border of the basal nucleus was already present from the definition of the medial border of the lateral nucleus. The paralaminar nucleus remains ventral to the basal

nucleus throughout most of the amygdala and the two nuclei are often difficult to distinguish. Therefore, for this study, the basal and paralaminar nuclei were combined into one contour and referred to as the basal nucleus. The ventral border of the basal nucleus was already present from the outer amygdala border outline.

In rostral sections, the outline of the basal nucleus began at the dorsolateral extent of the basal nucleus on the existing lateral border (Figure 2a). The outline then extended slightly dorsal to include the dorsal portion of the basal nucleus before continuing medially to complete the dorsal border. The outline continued ventrally to form the medial border of the basal nucleus until the existing ventral border of the amygdala was reached.

In more caudal sections, the basal nucleus increased in size (Figure 2b). The accessory basal nucleus formed the dorsomedial border with the basal nucleus and ventral to this, the basal nucleus was bordered medially by the periamygdaloid cortex. The ventromedial limit of the basal nucleus was associated with the medial extent of the paralaminar nucleus.

At midrostrocaudal levels, the dorsolateral portion of the basal nucleus was often encapsulated by white matter (Figure 2c). The outline was drawn from the dorsolateral extent of the main body of the basal nucleus on the existing outline as described above, continued to the dorsal tip of the main body, and extended to include the additional dorsolateral portion. The outline was drawn around the additional portion of the basal nucleus and continued back to the main body of the basal nucleus. The remaining outline of the basal nucleus was drawn as described above.

In more caudal sections, the basal nucleus decreased in size and the additional dorsolateral portion of the basal was fused with the main body (Figure 2d). The central nucleus was present at this level and separated from the dorsomedial portion of the basal nucleus by fibers.

In caudal sections, the amygdalohippocampal area replaced the periamygdaloid cortex as the ventromedial border of the basal nucleus (Figure 2e). The border between the amygdalohippocampal area and the ventral portion of the basal nucleus was often difficult to distinguish. Neurons of the amygdalohippocampal area were more homogeneously distributed, appeared darker, and more densely-packed than adjacent basal nucleus neurons. The medial extent of the basal nucleus continued to be defined by the medial extent of the paralaminar nucleus along the ventral surface of the amygdala. The outline at this level was drawn as described for rostral sections.

When the lateral nucleus was no longer present, the dorsal, lateral, and ventral borders of the basal nucleus formed part of the existing outer amygdala outline (Figure 2f). Surrounding structures included the central nucleus dorsally, accessory basal nucleus dorsomedially, temporal horn of the lateral ventricle laterally, and hippocampus ventrally. The outline of the basal nucleus at its caudal extent began at the existing outer amygdala outline, continued dorsomedially to the accessory basal nucleus, then ventromedially until the existing amygdala boundary was reached.

Delineation of accessory basal nucleus

The rostral extent of the accessory basal nucleus first appears dorsomedial to the basal nucleus (Figure 2b). The existing medial border of the basal nucleus forms the lateral border of the accessory basal nucleus. In general, accessory basal neurons are slightly smaller and more lightly stained than cells of the basal nucleus, and gradually decrease in size from dorsolateral to ventromedial. The periamygdaloid cortex was located medial to the accessory basal nucleus for the rostral two-thirds of the amygdala. The outline of the accessory basal

nucleus began at its dorsolateral extent at the existing basal nucleus outline. The outline continued medially around the dorsal extent of the accessory basal nucleus, then ventromedially along the fiber tracts, and completed along the ventral border until the preexisting outline of the basal nucleus was reached.

At midrostrocaudal levels, the accessory basal nucleus was bordered dorsomedially by the medial nucleus and medially by the periamygdaloid cortex (Figure 2c). The central nucleus was located dorsomedial to the accessory basal, but was clearly separated from it by fiber bundles. The dorsal and medial boundaries of the accessory basal nucleus were drawn as described above for rostral sections.

In more caudal sections, the accessory basal nucleus was bordered dorsolaterally by the central nucleus, dorsomedially by the medial nucleus, medially by the posterior cortical nucleus, and ventromedially by the amygdalohippocampal area (Figures 2d and e). The outline began at the dorsolateral extent of the accessory basal nucleus on the existing border of the basal nucleus as described in previous sections, continued dorsally around the dorsal tip of the accessory basal nucleus, continued medially and ventrally to the amygdalohippocampal area, then completed ventrolaterally to the previously defined lateral border.

In most cases, the accessory basal nucleus extended to the caudal pole of the amygdala and, at these levels, was nearly completely surrounded by fiber tracts (Figure 2f). At this level, the basal nucleus appeared more ventral than lateral to the accessory basal nucleus. The outline of the accessory basal nucleus at the caudal extent began at the existing basal nucleus outline along the ventrolateral border of the accessory basal nucleus, continued dorsally around the dorsal tip of the accessory basal nucleus, then ventrally until the existing basal nucleus outline was reached.

Delineation of the central nucleus

The central nucleus was located in the dorsocaudal portion of the amygdala, and was nearly completely encapsulated by fiber tracts. A band of fibers also separated the nucleus into two subdivisions. The lateral subdivision was made up of small, more lightly stained neurons relative to most of the amygdaloid complex, but homogeneous and densely packed. The polymorphic neurons of the medial subdivision stained slightly darker than the lateral subdivision and they were more loosely packed.

At the rostral extent of the central nucleus, the lateral division generally appeared before the medial division (Figure 2c). The dorsolateral portion of the basal nucleus was present ventrolaterally and the accessory basal nucleus was situated ventromedially. The dorsolateral border of the central nucleus was part of the outer amygdala outline. The remaining outline began at the most lateral extent of the central nucleus on the existing outline and continued ventrally, medially, then dorsally around the central nucleus until the existing outline was reached.

At midrostrocaudal levels, the central nucleus increased in size and both the lateral and medial divisions were present (Figure 2d). The dorsal surfaces of the accessory basal and basal nucleus formed a groove into which the central nucleus fit. The existing outer amygdala outline formed the dorsal and lateral border of the central nucleus. The central nucleus outline began at the ventrolateral extent of the central nucleus along the existing outer amygdala outline. The outline continued dorsomedially along the fiber tracts that separate the central nucleus from the basal and accessory basal nucleus, then dorsally along the lateral boundary of the medial nucleus until the existing outline was reached.

The caudal most section in which the total amygdala was traced was also the last section in which the central nucleus was outlined. The outer amygdala outline formed the dorsal and lateral borders of the central nucleus at this level. The remaining ventral and medial borders of the central nucleus were marked by the encapsulating white matter. The outline began at the ventrolateral extent of the central nucleus on the existing outer amygdala outline. The outline then continued medially and dorsally, along the white matter. The outline was completed along the white matter to the existing outer amygdala outline.

Delineation of remaining nuclei

The remaining amygdala nuclei were all other nuclei within the outer boundary of the amygdaloid complex that were not individually outlined. The remaining nuclei included the anterior cortical nucleus, anterior amygdaloid area, nucleus of the lateral olfactory tract, periamygdaloid cortex (Figure 2b), medial nucleus, posterior cortical nucleus, amygdalohippocampal area, and intercalated nuclei (Figure 2e).

Stereological sampling techniques

All measurements were made using a Nikon Eclipse 600 microscope attached to an Optronics camera with Microfire software (Goleta, CA), which was connected to a Dell Precision 450 workstation using Stereoinvestigator software (Microbrightfield, Inc, Williston, VT). The neuroanatomical limits of each of the regions were first defined, as described above, at low magnification with a 1× (0.04 NA) objective.

The volume of each region was estimated using the Cavalieri method. This tool is implemented by randomly overlaying a lattice of points over each section and then counting the number of points in the lattice that lie within the region being measured. A grid spacing area of .04 mm^2 (200 μm distance between points) was used to measure the area of each region. Volume was calculated by multiplying the area by the average measured section thickness for each region and subject.

An optical fractionator method was used to estimate the number of neurons in each subdivision of the amygdaloid complex at high magnification with a 100× (1.30 NA) oil objective (Figure 3). This technique involved counting neurons with optical disectors, a three-dimensional probe placed through a reference space (Gundersen, 1986;West et al., 1991). This method is independent of volume measurements and therefore unaffected by tissue shrinkage that takes place during any stage of tissue preparation. A neuron was counted if the nucleus associated with that neuron first came into focus within the optical disector counting frame (i.e. a neuron was not counted if the nucleus associated with that neuron came into focus within the guard zone or if the nucleus was touching the left or bottom side of the disector frame). The guard zone is an area at the top and bottom of the histological section in which neurons are not counted to avoid errors in estimation due to cutting artifact. Total section thickness was measured at every other counting frame site.

A pilot study of three cases was first carried out to determine an optimal sampling scheme. The precision of the estimate expressed as the coefficient of sampling error (CE) was calculated to determine the appropriate number and size of disector counting frames (Gundersen and Jensen, 1987; Gundersen et al., 1999). The CE is the variation in sampling within each individual and reflects the precision based on how intensely each individual is sampled. The CE may be improved by sampling more sections within each individual or sampling more disector sites within each section. Our goal was to reach a CE (Gundersen CE where m=1) of less than 10% (Gundersen and Jensen, 1987; Gundersen et al., 1999).

Optimal spacing of the counting frames (grid size) depended on the area of the amygdala subdivision being measured. The counting frame area (in μm^2) and grid size (in mm^2) for

each region is summarized in Table 2. The optical disector height (thickness) was 9 μm with a 3 μm top and bottom guard zone. Optimal disector and guard zone height was determined after measuring that the average post-processing thickness of the tissue ranged from 15-20 μm per section. The mean section thickness measured at each disector site was used for final calculation of neuron number for each subdivision of the amygdaloid complex. The estimation of neuron number was calculated by the product of the total number of neurons counted at the disectors, the section sampling fraction (number of sections/total area), the area sampling fraction (area of section sampled/total area), and the thickness sampling fraction (section thickness/disector height).

Results

Volume

The mean volume (mm^3), after all tissue processing was completed, of each subdivision of the human amygdaloid complex is summarized in Table 3. The coefficient of error (CE) was ≤0.01 for all regions measured. The volume of the total amygdaloid complex did not correlate with the age of the subject at death (Figure 4). Central nucleus volume was positively correlated with subject age at death ($p<.01$).

Neuron number

The mean number of neurons (10^6) for each subdivision of the human amygdaloid complex is summarized in Table 4. All coefficients of error (CE*(N)*) were ≤0.08. Neuron number did not correlate with the age of the subject at death in the total human amygdaloid complex or individual subdivisions (Figure 4).

Discussion

This study utilized modern stereological techniques to measure the total number of neurons in the human amygdaloid complex. There are approximately 12 million neurons in the human amygdaloid complex in subjects 11-44 years of age, with more than 50% residing in the lateral and basal nuclei. Previous studies have given qualitative descriptions of the human amygdaloid complex (Sorvari et al., 1995) and/or provided quantitative measures of neuronal density (Herzog and Kemper, 1980; Bauman and Kemper, 1985; Scott et al., 1992; Hudson et al., 1993; Bauman and Kemper, 1994; Wolf et al., 1997; Thom et al., 1999; Harding et al., 2002), but have not reported estimates of total neuron number. As a baseline for studies of pathology of the amygdala, density measures are problematic since differential shrinkage can occur at various stages of tissue processing and the shrinkage can vary with age at time of death (Haug et al., 1994; Pakkenberg and Gundersen, 1997). If tissue shrinks during processing, the number of neurons will not change, but there will be more neurons per unit volume. Design-based stereology has been used in other areas of the brain, such as the locus coeruleus, to refute earlier studies of age-related changes in neuronal density using assumption-based methods (Mouton et al., 1994; Ohm et al., 1997).

The only other study that we are aware of that carried out a quantitative stereological analysis of the human amygdala involved Alzheimer's patients (Vereecken et al., 1994). This study used a different definition of amygdala regions (Crosby and Humphrey, 1941) and an older patient population (mean age = 75.2 for controls). Interestingly, Vereecken and colleagues (1994) estimated fewer neurons in the overall amygdaloid complex in their older population of controls with 10.7 million neurons in the left (n=4) and 9.8 million neurons in the right (n=6). It would be of interest to conduct a stereological study on a larger sample of cases distributed throughout this age range to determine if there is an age-related decrease in

neuron number. The current study found that neither volume nor neuron number in the amygdaloid complex displayed a significant correlation with age in our subjects 11-44 years.

There are a few studies available that have utilized modern stereological techniques in other regions of the brain in order to compare our finding of 12.2 million neurons in the human amygdaloid complex. Pakkenberg and Gundersen (1997), using an optical disector technique, found that there are 23 billion neurons in the male neocortex, with 5 billion residing in the temporal lobe. Within the temporal lobe, West & Gundersen (1990) estimated the number of neurons in the hippocampal formation with an optical disector and found 15 million in the granule cell layer of the dentate gyrus, 2 million pyramidal neurons in the hilus of the dentate gyrus, 2.7 million pyramidal neurons in CA2-3, 16 million pyramidal neurons in CA1, and 4.5 million pyramidal neurons in the subiculum. West & Slomianka (1998) estimated the total number of neurons in the human entorhinal cortex using a similar optical fractionator technique that was used in our study. They estimated approximately 1 million layer II cells, 5 million layer III cells, 2 million layer V cells, and 4 million layer VI cells, for a total of 13 million neurons in the entorhinal cortex.

The intent of the current study was to demonstrate that stereological techniques can be used to estimate the number of neurons in subdivisions of the human amygdaloid complex. The use of the optical fractionator technique to estimate the total number of neurons required careful definition of the boundaries of each subdivision. However, few studies were available to serve as a guide for defining the extent of these regions. Therefore extensive explanation of the boundaries used in this study were provided. Future studies may also benefit from additional stains, such as myelin or acetylcholinesterase, to aid in the delineation of individual nuclei or even define subdivisions within each nucleus. Another technical modification that would enhance the current study would be to embed tissue in glycol methacrylate, rather than cutting frozen sections, to reduce the shrinkage of tissue (Dorph-Petersen et al., 2001). Although the optical fractionator technique eliminates consideration of biases related to tissue shrinkage, the thickness of our 100μm frozen sections were reduced by approximately 80% during processing. Embedded tissue would allow for the use of thinner sections for stereological techniques since shrinkage is reduced. Finally, this study demonstrates that it is possible to estimate absolute neuron number in nuclei of the human amygdaloid complex with an efficient sampling scheme, without the biases associated with density measures, in order to compare patient populations in which the amygdala may be pathological.

Acknowledgments

This work was supported by the National Alliance for Autism Research, the M.I.N.D. Institute and NIH grant MH41479. We wish to thank Gwyndolen Harburg for technical assistance, Dr. Jane Pickett and the Autism Tissue Program for facilitating tissue collection, and Geoff Greene at Microbrightfield and Dr. Pierre Lavenex for their thoughtful advice. Tissue samples were provided by the NICHD Brain and Tissue Bank for Developmental Disorders at the University of Miami (Director Carol Petito, M.D.). We are deeply indebted to the donors and their families who have made this study possible.

Literature Cited

Andersen BB, Fabricius K, Gundersen HJ, Jelsing J, Stark AK. No change in neuron numbers in the dentate nucleus of patients with schizophrenia estimated with a new stereological method--the smooth fractionator. J Anat. 2004; 205:313–321. [PubMed: 15447690]

Andersen BB, Gundersen HJ, Pakkenberg B. Aging of the human cerebellum: a stereological study. J Comp Neurol. 2003; 466:356–365. [PubMed: 14556293]

Bauman M, Kemper TL. Histoanatomic observations of the brain in early infantile autism. Neurology. 1985; 35:866–874. [PubMed: 4000488]

Bauman, M.; Kemper, TL. Neuroanatomic Observations of the Brain in Autism. In: Bauman, M.; Kemper, TL., editors. The Neurobiology of Autism. Baltimore, MD: Johns Hopkins University Press; 1994. p. 119-145.

Bowley MP, Drevets WC, Ongur D, Price JL. Low glial numbers in the amygdala in major depressive disorder. Biol Psychiatry. 2002; 52:404–412. [PubMed: 12242056]

Crosby EC, Humphrey T. Studies of the vertebrate telencephalon: II. The nuclear pattern of the anterior olfactory nucleus tuberculum olfactorium and the amygdaloid complex in adult man. J Comp Neurol. 1941; 47:309–352.

Dorph-Petersen KA, Nyengaard JR, Gundersen HJ. Tissue shrinkage and unbiased stereological estimation of particle number and size. J Microsc. 2001; 204:232–246. [PubMed: 11903800]

Gundersen HJ. Stereology of arbitrary particles. A review of unbiased number and size estimators and the presentation of some new ones, in memory of William R. Thompson. J Microsc. 1986; 143(Pt 1):3–45. [PubMed: 3761363]

Gundersen HJ, Jensen EB. The efficiency of systematic sampling in stereology and its prediction. J Microsc. 1987; 147(Pt 3):229–263. [PubMed: 3430576]

Gundersen HJ, Jensen EB, Kieu K, Nielsen J. The efficiency of systematic sampling in stereology--reconsidered. J Microsc. 1999; 193:199–211. [PubMed: 10348656]

Harding AJ, Stimson E, Henderson JM, Halliday GM. Clinical correlates of selective pathology in the amygdala of patients with Parkinson's disease. Brain. 2002; 125:2431–2445. [PubMed: 12390970]

Haug JS, Goldner CM, Yazlovitskaya EM, Voziyan PA, Melnykovych G. Directed cell killing (apoptosis) in human lymphoblastoid cells incubated in the presence of farnesol: effect of phosphatidylcholine. Biochim Biophys Acta. 1994; 1223:133–140. [PubMed: 8061045]

Herzog AG, Kemper TL. Amygdaloid changes in aging and dementia. Arch Neurol. 1980; 37:625–629. [PubMed: 7425886]

Hudson LP, Munoz DG, Miller L, McLachlan RS, Girvin JP, Blume WT. Amygdaloid sclerosis in temporal lobe epilepsy. Ann Neurol. 1993; 33:622–631. [PubMed: 8498843]

Korbo L, Amrein I, Lipp HP, Wolfer D, Regeur L, Oster S, Pakkenberg B. No evidence for loss of hippocampal neurons in non-Alzheimer dementia patients. Acta Neurol Scand. 2004; 109:132–139. [PubMed: 14705976]

Mouton PR, Pakkenberg B, Gundersen HJ, Price DL. Absolute number and size of pigmented locus coeruleus neurons in young and aged individuals. J Chem Neuroanat. 1994; 7:185–190. [PubMed: 7848573]

Ohm TG, Busch C, Bohl J. Unbiased estimation of neuronal numbers in the human nucleus coeruleus during aging. Neurobiol Aging. 1997; 18:393–399. [PubMed: 9330970]

Pakkenberg B, Gundersen HJ. Total number of neurons and glial cells in human brain nuclei estimated by the disector and the fractionator. J Microsc. 1988; 150(Pt 1):1–20. [PubMed: 3043005]

Pakkenberg B, Gundersen HJ. Neocortical neuron number in humans: effect of sex and age. J Comp Neurol. 1997; 384:312–320. [PubMed: 9215725]

Saper CB. Any way you cut it: a new journal policy for the use of unbiased counting methods. J Comp Neurol. 1996; 364:5. [PubMed: 8789271]

Schumann CM, Buonocore MH, Amaral DG. Magnetic resonance imaging of the postmortem autistic brain. J Autism Dev Disord. 2001; 31:561–568. [PubMed: 11814267]

Scott SA, DeKosky ST, Sparks DL, Knox CA, Scheff SW. Amygdala cell loss and atrophy in Alzheimer's disease. Ann Neurol. 1992; 32:555–563. [PubMed: 1456740]

Sorvari H, Soininen H, Paljarvi L, Karkola K, Pitkanen A. Distribution of parvalbumin-immunoreactive cells and fibers in the human amygdaloid complex. J Comp Neurol. 1995; 360:185–212. [PubMed: 8522643]

Thom M, Griffin B, Sander JW, Scaravilli F. Amygdala sclerosis in sudden and unexpected death in epilepsy. Epilepsy Res. 1999; 37:53–62. [PubMed: 10515175]

Vereecken TH, Vogels OJ, Nieuwenhuys R. Neuron loss and shrinkage in the amygdala in Alzheimer's disease. Neurobiol Aging. 1994; 15:45–54. [PubMed: 8159262]

West MJ, Gundersen HJ. Unbiased stereological estimation of the number of neurons in the human hippocampus. J Comp Neurol. 1990; 296:1–22. [PubMed: 2358525]

West MJ, Kawas CH, Stewart WF, Rudow GL, Troncoso JC. Hippocampal neurons in pre-clinical Alzheimer's disease. Neurobiol Aging. 2004; 25:1205–1212. [PubMed: 15312966]

West MJ, Slomianka L. Total number of neurons in the layers of the human entorhinal cortex. Hippocampus. 1998; 8:69–82. [PubMed: 9519888]

West MJ, Slomianka L, Gundersen HJ. Unbiased stereological estimation of the total number of neurons in thesubdivisions of the rat hippocampus using the optical fractionator. Anat Rec. 1991; 231:482–497. [PubMed: 1793176]

Wolf HK, Aliashkevich AF, Blumcke I, Wiestler OD, Zentner J. Neuronal loss and gliosis of the amygdaloid nucleus in temporal lobe epilepsy. A quantitative analysis of 70 surgical specimens. Acta Neuropathol (Berl). 1997; 93:606–610. [PubMed: 9194900]

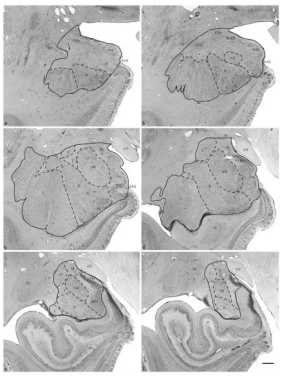

Figure 1.
Lateral view of the left hemisphere of the brain displaying the cuts made to obtain a tissue block of the intact amygdala. Scale bar: 1 cm.

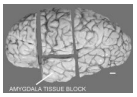

Figure 2.
Brightfield photomicrograph of Nissl-stained coronal section through (a, b) rostral, (c, d) midrostrocaudal, and (e, f) caudal amygdaloid complex. *Abbreviations:* (AAA) anterior amygdaloid area, (AB) accessory basal nucleus, (AHA) amygdalohippocampal area, (B) basal nucleus, (C) central nucleus, (COa) anterior cortical nucleus, (COp) posterior cortical nucleus, (EC) entorhinal cortex, (H) hippocampus, (I) intercalated nuclei, (L) lateral nucleus, (M) medial nucleus, (NLOT) nucleus of the lateral olfactory tract, (OT) optic tract, (PAC) periamygdaloid cortex, (PL) paralaminar nucleus, (PU) putamen, (SAS) semiannular sulcus, (VC) ventral claustrum. Scale Bar: 2 mm.

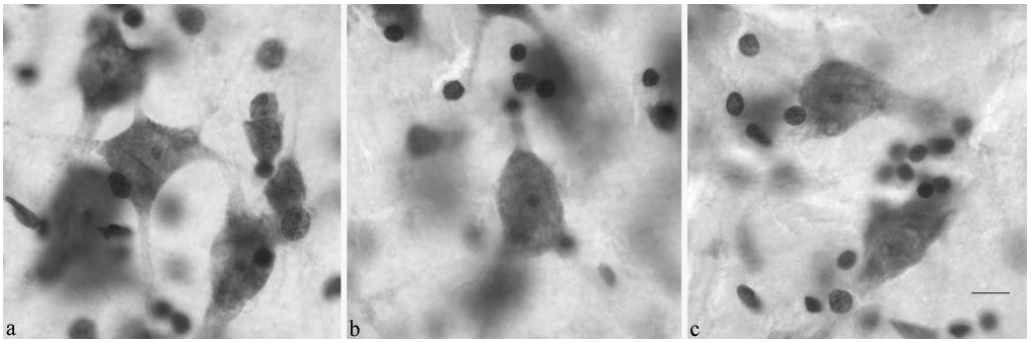

Figure 3.
Examples of tissue at 100×, the magnification used for the optical fractionator technique, from three cases: (a) 11 year old male in the left lateral nucleus, (b) 24 year old male in the right lateral nucleus, and (c) 44 year old male in the left lateral nucleus. Scale bar: 10 μm.

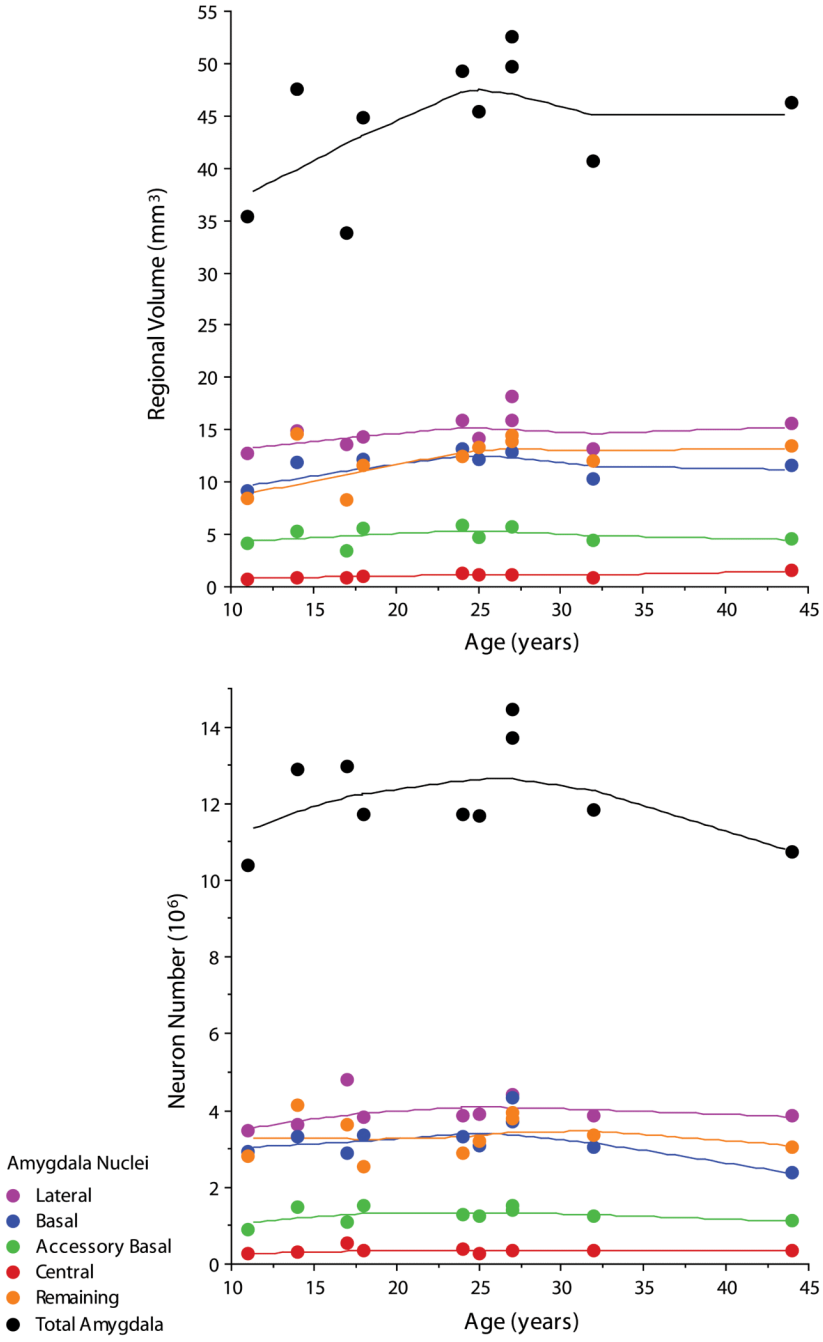

Figure 4.
Bivariate scattergram of volume (mm^3) and mean number of neurons (10^6) in each subdivision of the human amygdaloid complex by age (lines represent Lowess tension=80).

Table 1

Clinical characteristics of ten human cases in which the amygdaloid complex was analyzed.

Age at Death (in years)	Sex	Postmortem Interval (PMI in hours)	Hemisphere	Cause of Death
11	male	30	left	cardiac arrest / renal failure
14	male	19	right	drowning
17	male	24	left	motor vehicle accident
18	male	20	left	drowning
24	male	19	right	gunshot wound to chest
25	male	19	left	drowning
27	male	21	right	suicide by hanging
27	male	16	left	cardiac arrest
32	male	17	left	coronary arteriosclerosis
44	male	26	left	pneumonia

Table 2

Stereological sampling parameters for neuron number measurement with the optical fractionator method in each subdivision of the human amygdaloid complex.

Amygdaloid Complex Subdivision	Mean # of Sections	Disector Frame Area (μm^2)	Disector Grid Area (mm^2)	Mean # of Neurons Counted
Lateral Nucleus	17	3600	6.25	253
Basal Nucleus	20	3600	4.00	320
Accessory Basal Nucleus	18	3600	2.25	234
Central Nucleus	12	3600	1.00	158
Remaining Nuclei	20	3600	4.00	349

Table 3

Volume (mm^3) for subdivisions of the amygdaloid complex for each human subject after tissue processing. Mean volumes and standard deviation (SD) are also listed for each region.

Age (years)	Lateral Nucleus	Basal Nucleus	Accessory Basal Nucleus	Central Nucleus	Remaining Nuclei	Total Amygdaloid
11	12.70	9.13	4.13	0.77	8.52	35.34
14	14.94	11.90	5.28	0.93	14.57	47.58
17	13.57	8.26	3.40	0.89	8.24	33.83
18	14.28	12.18	5.53	1.06	11.54	44.85
24	15.90	13.11	5.84	1.22	12.52	49.22
25	14.15	12.16	4.72	1.08	13.34	45.38
27	15.91	12.85	5.67	1.17	14.41	49.68
27	18.21	13.90	5.75	1.21	13.93	52.50
32	13.20	10.25	4.48	0.91	12.09	40.72
44	15.57	11.56	4.60	1.53	13.45	46.27
MEAN	14.84	11.53	4.94	1.08	12.26	44.54
SD	1.63	1.79	0.81	0.22	2.26	6.13

J Comp Neurol. Author manuscript; available in PMC 2008 October 26.

Table 4

Number of neurons (10^6) for subdivisions of the amygdaloid complex for each human subject. Mean neuron number and standard deviation (SD) are also listed for each region.

Age (years)	Lateral Nucleus #	Basal Nucleus #	Accessory Basal Nucleus #	Central Nucleus #	Remaining Nuclei #	Total Amygdaloid #
11	3.462	2.943	0.913	.255	2.810	10.383
14	3.639	3.330	1.477	.318	4.136	12.899
17	4.799	2.903	1.106	.548	3.624	12.982
18	3.837	3.370	1.507	.360	2.543	11.718
24	3.871	3.302	1.276	.380	2.878	11.706
25	3.912	3.068	1.233	.288	3.191	11.692
27	4.333	4.329	1.506	.359	3.939	14.468
27	4.430	3.707	1.414	.351	3.802	13.705
32	3.855	3.034	1.234	.346	3.353	11.821
44	3.860	2.364	1.114	.349	3.061	10.748
MEAN	4.000	3.235	1.278	0.355	3.334	12.212
SD	0.401	0.524	0.199	0.078	0.529	1.282